Dynamics of salt marsh margins are related to their 3-dimensional functional form

Evans, B.R.; Möller, I.; Spencer, T.; Smith, G.

March 6, 2019

Abstract

The three-dimensional configuration of sedimentary landforms in intertidal environments represents a major control on regional hydrodynamics. It modulates the location and magnitude of forces exerted by tidal currents and waves on the landform itself and on engineered infrastructure such as sea walls or coastal defences. Furthermore, the effect is reflexive with the landforms representing an integrated, long-term response to the forces exerted on them. There is a strong reciprocal linkage between form and process (morphodynamics) in the coastal zone which is significantly lagged and poorly understood in the case of cohesive, vegetated sediments in the intertidal zone. A method is presented that links the geometric properties of the tidal flat-saltmarsh interface to the history and potential future evolution of that interface. A novel quantitative classification scheme that is capable of separating marsh margins based on their functional form is developed and is applied to demonstrate that relationships exist between landform configuration and morphological evolution across a regional extent. This provides evidence of a spatially variable balance between self-organised and external controls on morphodynamic evolution and the first quantitative basis for a quick assessment procedure for likely future dynamism.

1 Introduction

The strong feedbacks between sedimentary and hydrodynamic systems in the intertidal zone have been widely documented (Defina et al., 2007; Fagherazzi et al., 2004; van de Koppel et al., 2012) and highlight the

dynamic and highly functional nature of the topography within such systems. The characteristics of intertidal landforms have the potential to provide information both on the modification of hydrodynamic forces caused by the landform but also the process history at the location (unless this has been 'overwritten' by the effects of a high magnitude event (Cahoon, 2006)). Under an assumption of stationarity in the relationship between form and process, landforms perhaps also contain an indication of the 'process future', since their current configuration may be predictive of their ongoing geomorphic interaction with the hydrodynamic environment. At the large scale, as demonstrated here, marginal morphometry could have wider applications as a means of measuring landscape heterogeneity and micro-habitat or niche provision, in the study of ecosystem functioning and ecosystem service delivery over large areas.

Attempts have been made to categorise types of mudflat in conceptual (Dyer, 1998) and quantitative (Townend (2008); Dyer et al. (2000)) terms. No formal *functional* typology for vegetated upper tidal flat (saltmarsh) margins, analogous to the work of Dyer (1998) and Dyer et al. (2000) on mudflats, appears to have been attempted to date. Similarly, no quantitative descriptions of contrasting marsh margin configurations are currently available. When considering different landform configurations at the interface between the vegetated marsh and the fronting foreshore, discussions tend to be dominated by ideas of cross-shore slope and whether there is a cliff or scarp present. Allen (2000) discusses in a more explicit manner some of the differences between cliffed and ramped margins. He presents a genetic typology dividing ramped margins into three classes of origin but does not discuss their real-time functions within the system.

Explicit, quantitative landform descriptors are essential as a baseline measurement against which future three-dimensional changes in functional form may be assessed and predictions from morphological models may be validated. Quantitative description of landform characteristics also increases the variety and power of statistical methods available to investigate the nature of the interactions that occur at marsh margins (between hydrodynamics and sediment erosion, transport and deposition), their relative importance, effects and spatial distribution.

Fundamentally, the marsh margin represents the transition from an area too low in the tidal frame for vegetation to develop to an area high enough to be perennially vegetated. Within intertidal environments elevation exerts a primary control on vegetation establishment (Morris et al., 2002; Suchrow and Jensen,

2010; Marani et al., 2013; Roner et al., 2016). The vegetated margin therefore represents the spatial location of a critical elevation within the more general cross-shore slope.

A spectrum of margin slopes exists from gentle ramps extending tens of metres in the cross-shore to vertical scarps or cliffs where the cross-shore extent might be sub-metre (Allen, 1993). In addition to this variation a range of smaller-scale (metre or centimetre) topographic characteristics may be superimposed upon the general marginal slope (both along- and across-shore). These may include linear or non-linear topographic features creating sub-margin scale variations in elevation, slope and aspect. For cliffed cases, variations in planform complexity affect the range of orientations observed. In North West Europe, under conditions of moderate sea level rise characteristic of the late Holocene, marshes tend to develop such that the permanently vegetated marsh platform establishes a dynamic equilibrium close to the mean high water spring (MHWS) level (Allen, 1989) while inundation stress (Balke et al., 2016) or exposure (Gray et al., 1989) are too great for vegetation to survive much below mean high water neaps (MHWN). The consequence is that the marginal zone experiences regular inundation and a large variability in inundation depth; there is therefore likely to be a large variance in hydrodynamic conditions leading to diversity in the processes by which the landform affects hydrodynamics and vice versa. As a consequence Allen (2000) argues that the elevation range that characterises the vegetated margin is that in which erosional processes will be most prevalent.

To investigate the effects of morphodynamic interactions on landform evolution at landscape and decadal scales it is necessary to parametrise the manifestations of such interactions. To this end, broad categorisation of margin type is helpful if categories can be designed such that they separate different dominant processes, or dominant scales at which processes operate (which may be expected to lead to different system responses through time).

This study presents a conceptual typology for marginal landforms, the characteristics and functional influences of which are described. The potential for landform interaction with system processes is outlined. Morphometric methods are then developed that capture relevant landform attributes and result in a novel, quantitative, functional typology. Marginal form is then compared to observations of decadal-scale morphodynamics and instantaneous-scale hydrodynamic influences. The method also extends possibilities

for studies investigating, for example, relationships between marsh edge habitats, faunal assemblages and ecosystem service provision by providing a quantitative description of a major structural component of the habitat that may support the development of niche models (e.g. Whaley and Minello (2002); Minello et al. (1994); Baltz et al. (1993); Glancy et al. (2003)).

1.1 Conceptual functional typology

A classification of marsh margins into three categories is adopted within this study, based on the consideration of three distinct process environments associated with their marginal geometries. There has been little attention given to the relationship between margin geometry and evolutionary tendencies, with this literature hitherto limited to modelling of marsh cliff formation and subsequent erosion (van De Koppel et al., 2005; Singh Chauhan, 2009). Both diversification and validation would therefore be desirable additions to the debate.

The three margin types (ramps, cliffs and ridge-runnel) identified by Allen (1993) are adopted by this study. These are represented schematically with photographic examples in Figure 1. The different end-member landforms identified above can be expected to modify and respond to local hydrodynamic conditions in differing ways which in turn will affect their morphological evolution. The landform interactions with hydrodynamics operate at an instantaneous timescale while measurable morphological evolution can only be considered at decadal timescales. This disjuncture is challenging but the morphometric approach used here supposes that between-class differences in the nature of instantaneous interactions, additively realised over decades, will produce measurably different morphological trajectories. The principal landform attributes that may describe instantaneous interactions are cross-shore slope, landform alignment and topographic complexity. For the purposes of this study, 'landform alignment' is used to refer to the relative dominance of slope directions between those that are shore-aligned and those that are shore-normal, at the scale of landforms spanning a number of 25cm pixels. 'Topographic complexity' is used to refer to the magnitude and frequency of elevational changes, again at a scale that can be evaluated with a pixel size of 25cm.

Ramped margins have a shallow slope and are therefore the most spatially extensive transition between marsh and tidal flat but with little or no sub-margin scale topographic variation. Characterised by gradual

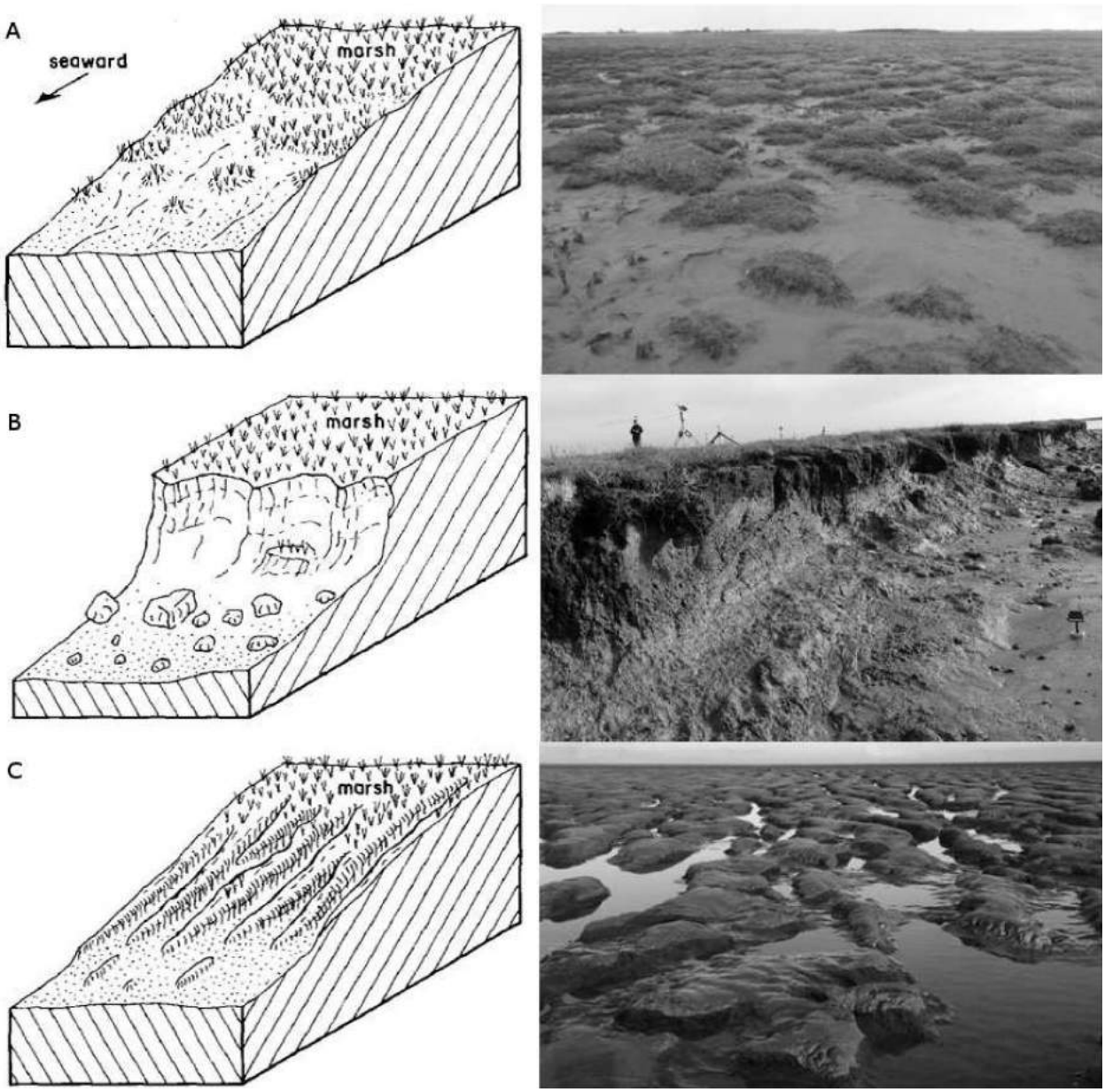

Figure 1: Margin types identified as common within the UK. (A) ramped transition with patchy vegetation (Donna Nook, Lincolnshire). (B) marsh cliff (Abbotts Hall, Essex). (C) ridge-runnel (Tillingham, Essex). Schematics adapted from Allen (1993). Photograph credit: A - Ben Evans, B and C - James Tempest

changes in elevation, ramps are highly dissipative features likely to result in the lowest maximum shear stresses being experienced at the sediment surface of any of the landform types. Current flows are likely to be relatively uniform and two-dimensional. Refraction and wave energy attenuation may also be uniform. Sediment mobilisation again depends on shear stress, which is related to the wave height to water depth ratio. If energy is low or sediment loads high and deposition occurs there are limited factors that might lead to preferential accretion in particular locations. Once vegetation or biofilms become established and the feedbacks associated with those developments begin to have an effect, the fine-scale (metres) topographic variability tends to increase (e.g. Temmerman et al., 2007). Given the difficulty in finding vegetated margin zones conforming to a true planar slope this class is more realistically represented by a morphology with some degree of low-amplitude topographic variability superimposed on the underlying cross-shore slope (See Figure 1).

Cliffs are the most abrupt and shoreline-aligned marginal transition, being characterised by a scarp, which may exceed 1m in height (e.g. Leonardi and Fagherazzi, 2014). These tend to act as reflectors of wave energy while the water level is between the base and top of the cliff. In the absence of an armouring effect from the persistence of blocks produced by earlier marsh edge failure (Gabet, 1998), the result is the greatest concentration of wave energy of any of the margin types and therefore an increased probability of exceeding the critical shear strength and mobilisation of sediment. Tonelli et al. (2010) find that forces exerted by waves are higher for vertical cliffs than for terraced ones. The vertical faces of cliffs do not tend to allow the establishment of vegetation or other biofilms to increase the stability of the sediment (van De Koppel et al., 2005). They are thus expected to be particularly vulnerable to erosion. Once water levels overtop the marsh platform, forces on the face decrease (Tonelli et al., 2010) and the cliff begins to act to both reflect and shoal waves, with a proportion of the wave energy propagating beyond the margin depending on wave height to water depth ratios (Möller and Spencer, 2002). Under most conditions these landforms do not produce regions of low hydrodynamic energy in front of them at the instantaneous timescale and are therefore principally erosive features which will continue to retreat once formed. Over longer timeframes eroded material may become deposited on the fronting mudflat (hydrodynamic conditions permitting), raising its elevation and increasing energy dissipation. This may gradually lead to sufficient energy absorption to

halt cliff retreat and the feature becoming relict (Allen, 1989). Fronting mudflats may also widen through marsh retreat, either enhancing energy dissipation and reducing erosion (Mariotti and Fagherazzi, 2010) or increasing fetch, thereby enhancing wave power and, consequently, erosion (Marani et al., 2011; Mariotti and Fagherazzi, 2013; Leonardi et al., 2016).

Ridge-runnel describes a transition type that is of intermediate cross-shore slope but characterised by topographic variability of significant amplitude relative to the elevation change over the transition zone and landforms that are largely shore-normal in alignment. Little work has been done to investigate formation of, and processes within in ridge-runnel systems of saltmarshes. The work of Priestas and Fagherazzi (2011) on similar landforms that they term wave-cut gullies, may provide some insight into the evolution and hydrodynamic processes that form and perpetuate such landforms. The gullies that they study are isolated, whereas ridge-runnel tends to comprise a repeating alongshore pattern of similar structures. Gullies may therefore represent an intermediate morphology between cliff and ridge-runnel. The hydrodynamic effects of (and on) spur and groove morphologies in coral reef systems have, however, been studied for many years (e.g. Roberts et al. (1975, 1992)). Such systems bear striking similarities to ridge runnel landforms, although the scale can be substantially greater. Some inferences regarding hydrodynamic-landform interactions may therefore be drawn from findings in coral reef contexts alongside broader saltmarsh literature. For deep water depths and long wavelengths the ridge-runnel topography may modify the hydrodynamics at the interface in a similar manner to the ramped margin, i.e. relatively uniformly and dissipatively since the topography acts as an enhanced roughness for waves with lengths exceeding the topographic length scale. As water depths decrease, or wave heights increase, the amplitude and wavelengths of the ridge-runnel features will lead to substantially different wave-bed interactions compared to a ramped margin. Recent hydrodynamic modelling in spur and groove systems has shown that the topography drives local circulation cells under conditions where the wavelengths of landform and incoming waves are such that diffraction leads to alongshore variations in wave height (Rogers and Monismith, 2014).

The three-dimensional flow fields are likely to be complex with small-scale refraction and reflection processes leading to a high spatial heterogeneity in energy concentration and the vectors of those forces are likely to be less uniformly shore-normal than for a ramp or a cliff, representing a potential feedback that

reinforces the landform heterogeneity. During specific points in the tidal cycle flows become channelised in a shore-normal direction, with localised enhanced long-shore flows from ridge to runnel. Erosive and depositional environments may be found in close proximity with a high degree of temporal variability also being apparent.

2 Methods

2.1 Marginal morphometry and classification

Marsh edge morphologies were investigated on the coastlines of East Anglia, UK (Figure 2). Field observations and aerial photographic interpretation indicate that marsh margins adopt a limited number of characteristic forms within this study region and that they are broadly similar to those observed elsewhere (Allen, 2000), and described above.

The marsh margin, defined as the point of transition between vegetated and un-vegetated foreshore, was manually digitised from Environment Agency true colour aerial photography with a pixel size of 25cm, acquired in either summer 2013 (Essex) or summer 2014 (Suffolk and Norfolk) and represented as a polyline. The same marsh margin line was used for the change detection analysis (section 2.2), ensuring co-location of morphometry and change data whilst maintaining methodological comparability. For the purposes of this study the marsh margin, as determined for 2013-2014, was assumed to be adequately representative of the marginal position in 2008 when LiDAR data were acquired. In order to fully automate the workflow, an automated classification allowing for determination of marsh edge location would have been ideal. This challenge is non-trivial, however, and was beyond the scope of this project. The challenges associated with automating this stage of the process, and justifications for using a manual vectorisation approach, are further detailed in the supplementary material.

The shoreline vector was then passed to an automated process (in Arc GIS 10.2) to compute morphological parameters at the marsh margin based upon composite LiDAR DTM data with 25cm pixel size, acquired in summer 2008 as part of a strategic monitoring programme by the Environment Agency (http://environment.data.gov.uk/ds/survey). The initial stages conducted for this analysis are represented

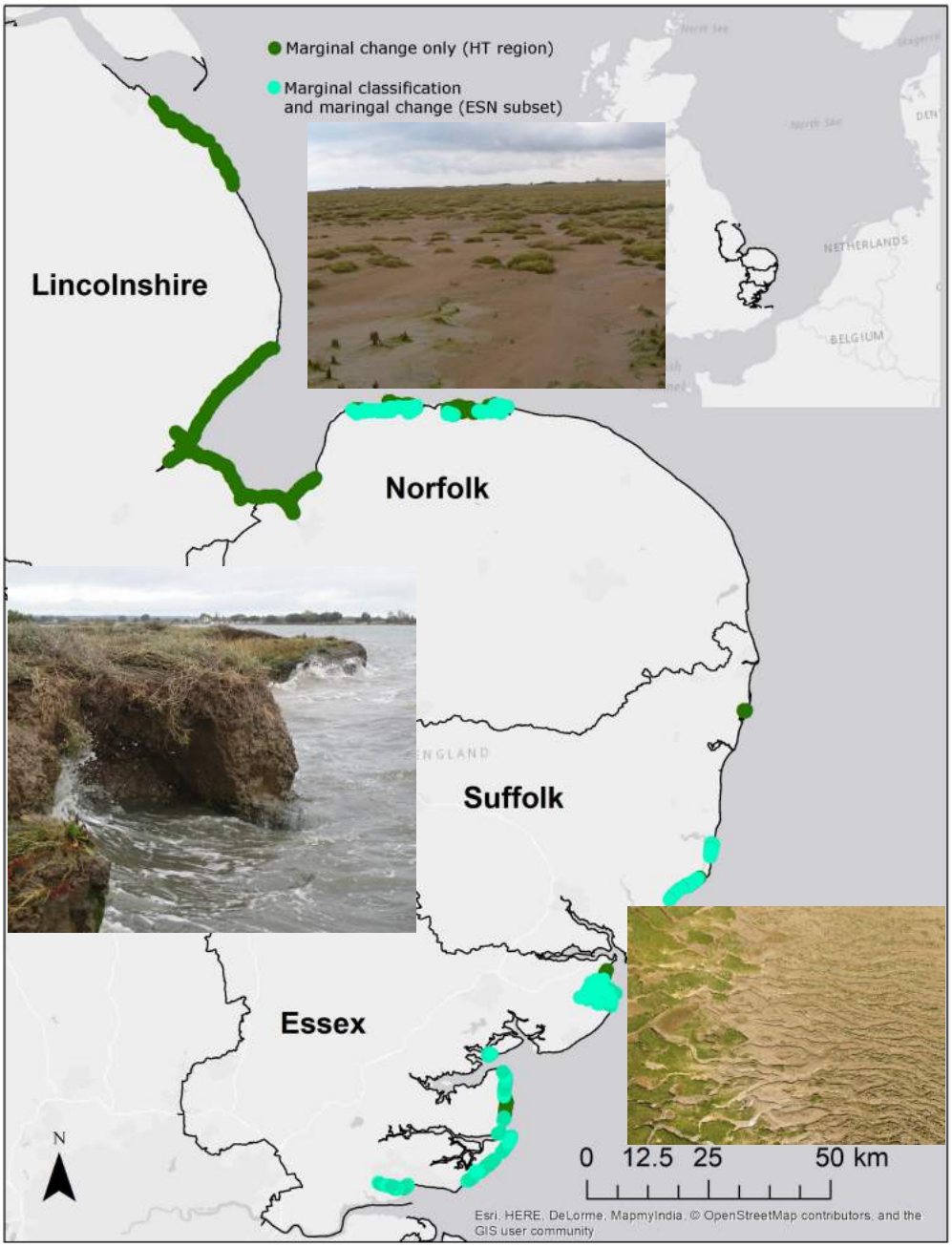

Figure 2: Location of study showing regional coastline of East Anglia comprising four coastal counties (Essex, Suffolk, Norfolk and Lincolnshire). Data coverage upon which analyses are based is indicated, with the parts of the region between The Humber and The Thames for which marginal change estimates were available being denoted HT, and the subset for which it was also possible to classify margin types being denoted ESN. Photo inserts: Top - ramped margin, Lincolnshire (B. Evans), Middle - cliffed margin, Essex (I. Möller), Bottom - ridge-runnel margin, Essex (B.Evans)

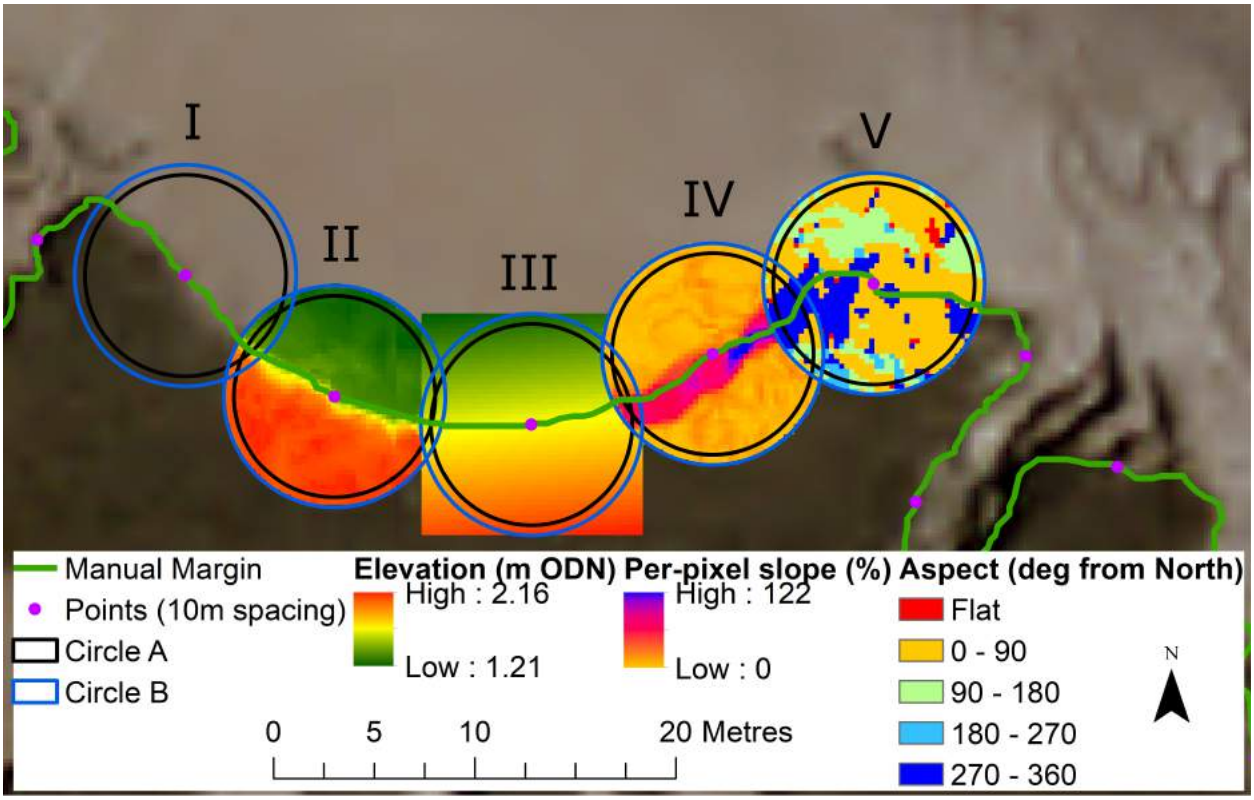

Figure 3: Initial geoprocessing stages for morphometric analysis superimposed upon 2013 aerial photograph of a section of marsh cliff (Essex). Manually-digitised shoreline vector is shown in green, with points established at 10m intervals along it. I=circles A and B, II=LiDAR elevation, III=elevation of first order surface, IV=per-pixel slope and V=per-pixel aspect in degrees from North.

in Figure 3. Points were created along the margin polyline, separated by a user-specified step distance that allows sampling density to be varied according to requirements. In this case a step distance of 10m was used. A circle of specified radius (10m here, equating to approximately 1250 pixels of the 25cm LiDAR raster) was then buffered around each point. For each such circle (henceforth "circle A"), a second circle ("circle B") was defined (I in Figure 3), having a diameter equal to that of the original circle plus four pixel widths (i.e. +1m for the 25cm DEM - II in Figure 3). This additional buffering avoids edge effects relating to some treatments of the raster data such as calculation of pixel slope and aspect, which require a full complement of adjacent pixels.

The cross-shore slope of the marginal zone was described by fitting a first order (least-squares) surface through the DEM for circle B (III in Figure 3) and computing its slope (%) and aspect (to determine shoreline orientation) within circle A. The shoreline azimuth was taken as perpendicular to the aspect and

was used to denote the offshore direction (approximately North in Figure 3).

A normalised-difference orientation index (NDMOI) was developed to describe the alignment of marginal landforms relative to the shoreline azimuth. Slope (%) (IV in Figure 3) and aspect (V in Figure 3) relative to the shoreline azimuth (degrees) were computed for each pixel of the LiDAR DTM within Circle A, based on the DEM of circle B. Masks were then computed identifying pixels whose aspect is broadly aligned (±45 degrees) to the shoreline azimuth and those that are broadly perpendicular to it (±45 degrees of shoreline aspect). Assuming that greater slopes describe more functionally significant topographical variation (in terms of hydrodynamic interactions), the sum of slope values for each class of pixel (aligned ($\Sigma_{S\_aligned}$) or perpendular ($\Sigma_{S\_perpendicular}$) was calculated. To provide a stable and readily interpreted index of landform-to-shoreline alignment, a normalised difference transformation was applied to the sums of slopes (Equation 1). The resulting index is in the range -1:1, with positive values indicating a dominance of landform alignment perpendicular to the shoreline (e.g. shore-normal ridge-runnel systems) and negative values indicating a dominance of shore-aligned landforms (e.g. a linear cliff).

$$NDMOI = (\Sigma_{S\_aligned} - \Sigma_{S\_perpendicular})/(\Sigma_{S\_aligned} + \Sigma_{S\_perpendicular}) \quad (1)$$

Topographic complexity, amplitude, and the frequency of different magnitudes of elevation change were represented by the kurtosis of the frequency distribution of per-pixel slopes within circle A. In order to remove the confounding influence of variable ranges of slope values over which kurtosis was calculated, frequencies were computed for slopes in the range 0-100% with a bin width of 5%. The bin size and number of bins (and therefore the overall range of slopes considered) were tunable parameters, but 20 bins of width 5% were found to provide good separation between the desired classes. Examples of relevant values, for individual example locations representing each end-member type, are shown in Figure 4. Kurtosis values of the distributions shown in panel C are: ramp=15.73; cliff=0.22 and ridge-runnel=-0.18.

For each circle A (ca. 1250 pixels), the process also derived other zonal statistics describing the morphology represented by the LiDAR DTM. These included minimum elevation, maximum elevation, elevation range, skewness of the slope distribution and the median absolute difference (Trevisani and Rocca, 2015). Exploratory analysis of the results showed that these supplementary zonal statistics provided little added

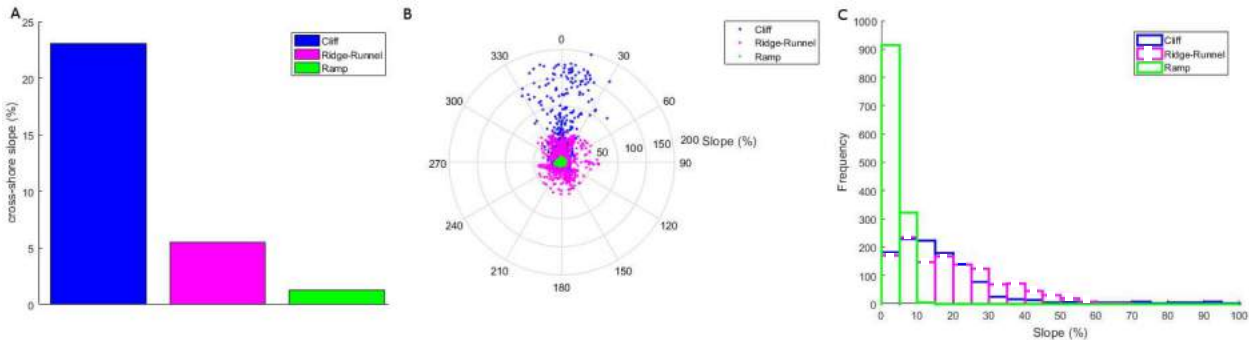

Figure 4: Comparison of margin type indicators for example 10m diameter circles representative of each class based on their position within the parameter space . (A) first-order slope through DEM points. (B) Distribution of per-pixel slopes and aspects relative to shore-aligned (polar axis, 0 degrees). (c) frequency distribution of per-pixel slopes

separation between different marginal landform types. Sensitivity tests were conducted to assess the effect of sampling area on discrimination of these types. The comparison showed that a 10m diameter sampling circle maximised overall parameter-space separation. Smaller circles suffered from insufficient sampling points (taken from a 25cm raster) to properly constrain the distribution of between-pixel slopes that described topographic complexity. Smaller circles are also more vulnerable to location errors relative to the topographic margin arising from the manual digitisation procedure and the temporal mismatch between the imagery from which margin location was derived and the DEM being sampled. This means that there is a higher probability of smaller sampling circles not actually sampling the margin but falling either landward or seaward of it. Larger circles resolved differences in cross-shore slope poorly because they incorporated too much non-marginal (and therefore essentially flat) topography.

A three-class unsupervised (k-means) classification of the entire dataset was carried out to objectively separate the landform types based on their slope, landform alignment and topographic complexity.

The classification was applied to marsh margins in Norfolk, Suffolk and Essex at an along-shore spacing of 10m, resulting in 41449 margin type classifications.

For this particular study validation is problematic. No formal typology of margins exists against which an unequivocal validation could be conducted. While Allen (1993) describes characteristics defining distinctive margin types, no attempt is made to map or quantify these. There is therefore no 'benchmark' against which to compare the classifications derived here, and certainly no previous quantitative typology against which to validate findings. In order to estimate classifier performance, regions were manually identified that

were considered, based on field and aerial photographic observations, to be overwhelmingly dominated by a given margin type. Classifications within these regions were assessed. Only one region was deemed to be characterised almost exclusively by ridge-runnel morphology (Tillingham, Essex), coverage of which was limited by lack of LiDAR data for some of the area. Consequently the validation set for ridge runnels was considerably smaller than for the other two classes (n=47). A total of 683 classified circles (A) were used for validation. Manually determined margin type was compared to classification outputs. The overall correct rate was 0.82, with a sensitivity (true positives rate) of 0.71 and specificity (true negatives rate) of 0.95.

2.2 Changes in margin position

Lateral marsh morphodynamics were represented by the change in position of the marsh margin over time. The marsh margin was defined as the point of transition from vegetated to un-vegetated substrate. The aim was to achieve the longest possible interval over which to measure change using comparable datasets of similar spatial resolution. The dataset chosen for analysis of marginal position was therefore the Environment Agency aerial photography. The baseline year (t0) was chosen as the first for which a relatively comprehensive survey of the coastline in question was acquired, namely 1992. The second comparison year (t1) was chosen as the most recent dataset available at the time the analysis was started. For Essex this was acquired in 2013, while for the rest of East Anglia it was 2014. The 1992 imagery was panchromatic with a 25cm pixel, while the 2013/14 imagery was four-band (including infrared) at 20cm resolution.

Aerial surveys were conducted in late summer/early autumn and as such represent the period of maximum seasonal growth on the marshes. The transition from vegetated to un-vegetated surfaces is therefore likely to represent the limit of annual rather than perennial vegetation in cases where the shoreline profile is such that these two differ. Manual digitisation of marsh margins based on visual assessment of the aerial photography offered a consistent methodology across datasets of different spectral characteristics and a robust and accurate determination of the position of the marsh margin. Baily and Pearson (2007) opted for a similar methodology when seeking to estimate changes in marsh extent on the South coast of the UK as did McLoughlin et al. (2015) in Virginia, USA.

For each year (1992 or 2013/14), the aerial photographs, supplied by the Environment Agency as or-

thorectified and colour-balanced images, were imported into ArcMap 10.2 (ESRI) and the marginal position was then digitised using a graphics tablet (UGEE M708). Digitisation was conducted with the imagery zoomed to greater than 1:500 as a compromise between having sufficient contextual information to locate the margin and minimising errors relating to manual precision.

Errors related to interpretation of margin location were estimated by repeat digitisation (n=10) of 2.5km long subset regions on different days. Errors related to the precision with which the desired shoreline vector could be drawn were estimated by multiple tracing (n=10) of an existing vector along the same sections. Differences between vectors were calculated at 10m intervals using the 'near' functon within ArcGIS. Interpretation errors were found to differ based on margin type and are reported in Table 1. Tracing errors had a root mean square error (RMSE) of 0.27m and coefficient of variation (CoV) of 0.99m. Image co-registration errors were estimated using 62 control points across the region. RMSE was 1.22m and CoV 0.83m. No systematic direction of error was identifiable. Errors were found to be highest where margins were most dynamic, which meant that signal-to-noise ratios typically remained low in these locations (see results section).

Regional coverage was typically good on the open coast and in outer estuarine areas but poor in inner estuaries such as those of Essex and Suffolk. This introduces a degree of sampling bias by excluding some of the more sheltered and fluvially-affected parts of the marsh system. Creek margins were digitised for creeks exceeding 20m width. Following digitisation of the marsh margins for both time periods, the change in position was estimated using the Digital Shoreline Analysis System (DSAS) (Theiler et al., 2008). DSAS is an extension for ArcGIS that estimates the Shoreline Change Envelope (SCE (m)) and End Point Rate (EPR (my^{-1})) by calculating the intersections of datestamped shorelines with shore-normal transect lines cast from a baseline. DSAS transects were cast at 10m intervals along the baseline and were manually filtered to exclude those approaching the shoreline obliquely (>45°) as a result of the high planform complexity of the marsh systems. A total of 33287 shoreline change estimates were thereby derived, covering the coastline between The Humber and The Thames (henceforth referred to as HT - see Figure 2).

LiDAR coverage only extended to the marsh margins in Essex, Suffolk and Norfolk and was not comprehensive within these counties. Margin classifications at 10m intervals were associated with lateral change

rates by executing a spatial join between the centrepoint of each DSAS transect (clipped to the SCE) with the nearest centroid of a margin classification circle. A maximum search radius of 20m was used to ensure that only nearby marginal classification data were extracted. Volumetric change rate (VCR) estimates were obtained by combining lateral migration rates with elevation ranges calculated during margin type classification. Two assumptions were required; that landform types are consistent through the period of observations (McLoughlin et al., 2015) and that elevations in the 10m sampling diameter are representative of the cross-shore range of elevations at the margin. This resulted in a dataset of 15774 paired margin type and change estimates (this subset henceforth referred to as ESN - see Figure 2).

2.3 Exposure of margin

The ESN subset was additionally divided into locations that were exposed and those that were sheltered. The criterion applied was whether the margin location has uninterrupted (by marsh platforms represented in the Phelan et al. (2011) dataset or by land masses) line of sight to any point 10km offshore. 'Exposed' is henceforth used to denote those margins with a line of sight to any point 10km offshore, whilst 'sheltered' denotes those that do not. The analysis was conducted in Arc GIS 10.2 using the 'viewshed' tool.

3 Results

Proportions of margin classes within the ESN subset were 20.1% ramps (n=3166), 48.8% cliffs (n=7705) and 31.1% ridge-runnel (n=4903). These were very similar to the overall set of margin classifications, including those not associated with change estimates, for which 20.5% were ramps(n=8507), 46.1% cliffs (n=19100) and 33.4% ridge-runnel (n=13824).

Table 2 compares descriptive statistics for marginal change rates across the entire HT regional extent to those for the subset of locations with margin classes (ESN) and the exposed and sheltered locations within the ESN subset. Histograms of all four populations are shown in Figure 5.

In Matlab one-way ANOVA followed by a multiple comparison test using the 'multcompare' function was used to test for differences in the mean EPR and VCR between margin classes for the ESN subset. Tests were replicated for the exposed and sheltered locations within ESN. Both signed and absolute quantities for

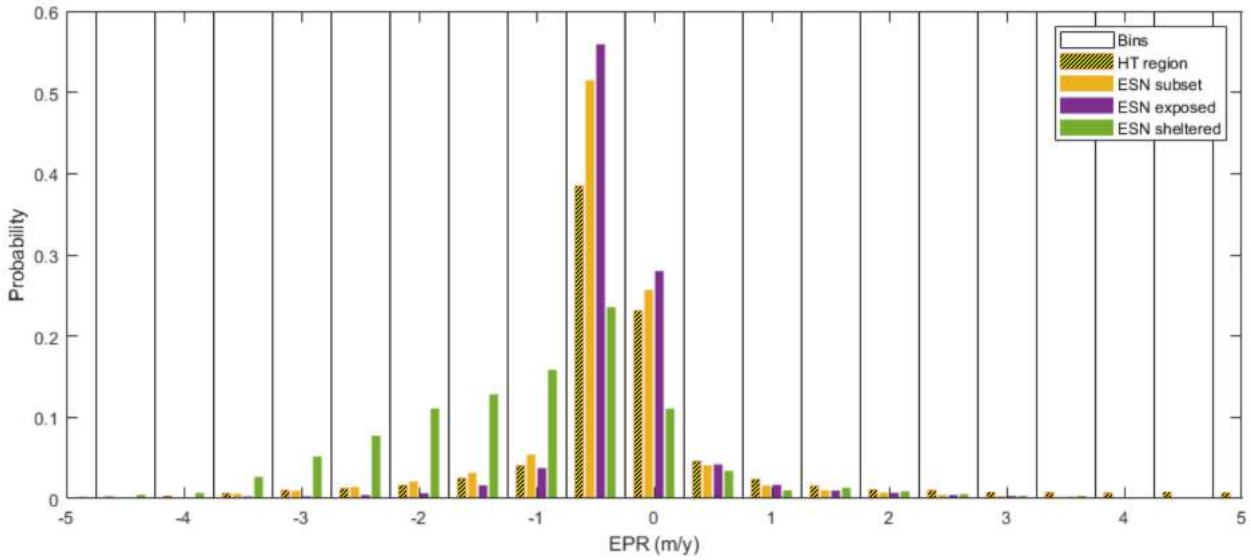

Figure 5: Probability distributions of EPR for entire HT region, ESN subset, Exposed and Sheltered locations within the ESN subset

each change metric were tested. The Scheffe procedure was selected as the most conservative option suitable for unbalanced sample sizes. Results of the multiple comparison tests are presented in Figure 6 and Table 3.

3.1 Planimetric changes

Over the HT region we find a mean advance of marsh margins by 2.42 m/y, albeit with high variability (SD 6.85m). In comparison, for ESN only, there is mean retreat at -0.1 m/y (SD 0.88m). Rapid advance of marsh margins is observed in The Wash embayment, with a maximum rate of progradation of 75.78my^{-1}. It is the widespread and rapid vegetation establishment in this area that is responsible, in large part, for the increased range and standard deviation compared to ESN, and this results in a more positively skewed and leptokurtic distribution of EPR. The contrast between a maximum retreat of 10.95 m/y and advance of more than 75 m/y is striking. Both HT and ESN regions show positive skew around medians very close to zero, which also implies a tendency for advance to outpace retreat. In exposed settings (section 2.3) we see strong mean retreat but retain positive skewness for all margin types with the notable exception of cliffs. For sheltered environments the median retreat is again very close to zero and the population is positively skewed. This implies that cliffs in exposed locations are the only context in which we observe retreat rates typically to outpace rates of advance.

Within the ESN region, all margin types demonstrate a tendency towards retreat, reflecting an overall erosive trend. Results show that, in terms of lateral migration rates, the behaviour of the three classes is significantly different with ramps, on average, retreating fastest ($0.23 my^{-1}$). Cliffs have the lowest lateral retreat rates (EPR, row A in Figure 6), with ridge-runnels exhibiting intermediate behaviour. Ramps retreat with a mean rate approximately two and a half times that of ridge-runnels and nearly five times that of cliffs.

For exposed settings EPR becomes strongly negative (erosive) across all margin types with cliffs exhibiting significantly slower retreat than the other two classes. In sheltered conditions ramps and ridge-runnels become slightly accretional on average while cliffs remain very slightly erosional ($-0.01 my^{-1}$). Magnitudes of mean change are an order of magnitude smaller than for exposed contexts. External forcing, in terms of hydrodynamic exposure, therefore appears to be more important than any morphodynamic feedback signal for controlling decadal-scale changes in margin position.

When the absolute EPR, a measure of lateral dynamism, is considered (row B in Figure 6) the results show that, over the ca. 20 year time period of change assessed here, ramps are much more dynamic than ridge-runnels which in turn are more dynamic than cliffs. This pattern holds for both exposed and sheltered environments, with all classes being less dynamic when sheltered than the least dynamic class (cliffs) when exposed. Geomorphic context and energy exposure therefore appear to strongly influence the potential for lateral changes observed at marsh margins (Leonardi and Fagherazzi, 2014). This concurs with previous work that has identified a linear relationship between marsh edge retreat and wave power (Marani et al., 2011; Leonardi et al., 2016).

3.2 Volumetric changes

When the signed VCR (row C in Figure 6) is considered, volume changes in cliffs and ridge-runnels are no longer significantly different across ESN, while changes at ramped margins remain separable from, and significantly more negative than, the other classes. This implies that, although the rates of change in margin position may be substantially different between cliffed and ridge-runnel margins, the volumes of sediment exchanged during migration of these landforms are similar. Exposed cliffs become the most volumetrically

erosive type, moving significantly more sediment than ramps. Therefore, while they may be apparently the most stable landform in terms of EPR, when exposed to high energy they exhibit the greatest rate of sediment mobilisation (geomorphological work), which confirms previous claims to their efficiency at concentrating energy (e.g. van De Koppel et al. (2005)). Cliffs are also the most erosive features in terms of VCR for sheltered environments, which aligns with their negative EPR. Importantly, sheltered VCR is also negative for ramps and ridge-runnels, despite their EPR being positive. This demonstrates that, in low energy conditions, it is the steeper examples of these landforms that retreat while those with shallower cross-shore slopes tend to prograde.

Dynamism, as represented by absolute VCR (row D in Figure 6), appears to be greatest for ramps and smallest for cliffs across the ESN subset. In exposed settings, however, ramps show the lowest dynamism, while volume changes in cliffs and ridge-runnels are substantial (exceeding $1 m^3 y^{-1}$) but very similar between classes. For sheltered regions the mean absolute volumetric changes show no significant differences between any of the margin types.

4 Discussion

4.1 Distribution of margin types

The inventory facilitated by the typology developed here demonstrates that, within the ESN region, margin types are not evenly distributed. Cliffs are the most common type, followed by ridge-runnels, with ramped margins being relatively rare. The relative paucity of ramped margins arises since, as previously noted, planar slopes tend not to persist at marsh margins since vegetation presence or establishment leads to increased topographic complexity (Temmerman et al., 2007). The ramped class, therefore, may not represent a morphodynamically stable condition. The dominance of cliffed margins suggests, in contrast, that these are a relatively stable (persistent) marginal form. The high membership of the class referred to here as ridge-runnel is disproportionate to the presence of these landforms based on visual assessment of the region. This is because the classification includes within this category many relatively isolated areas where the planform of the margin is complex within the 10m scale of the morphometric calculations. Such areas are typically creek

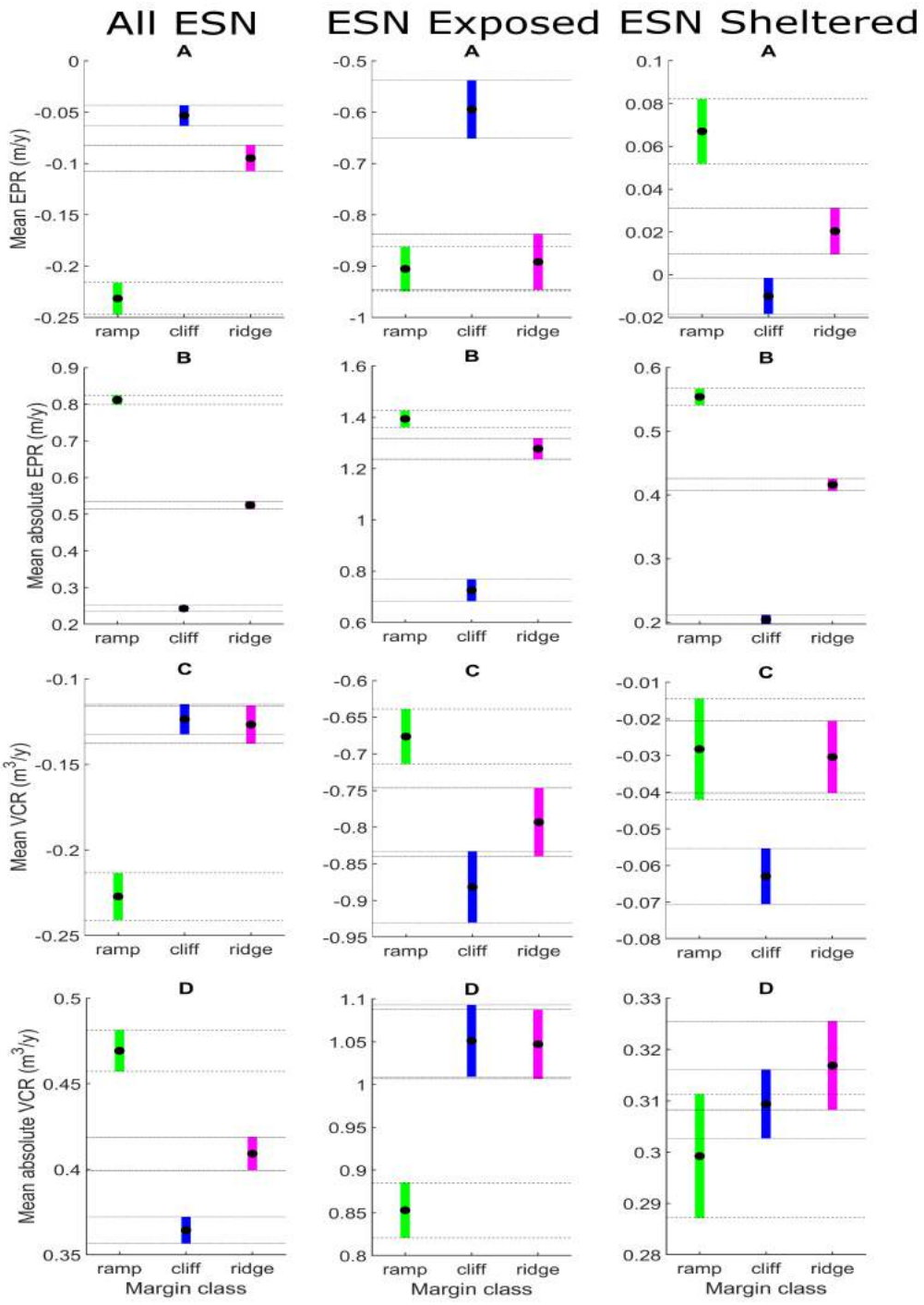

Figure 6: Multiple comparison of mean margin type behaviours for the entire ESN region (top panel) in addition to exposed (middle panel) and sheltered (bottom panel) locations within it. A: EPR, B: Absolute EPR, C: VCR, D: Absolute VCR. Horizontal dashed lines indicate one standard error. Note that y-axis scales vary between panels for clarity. 'ridge' denotes ridge-runnel

intersections, abrupt channel meanders or areas where smaller (≈5m wide) creeks are present. Examples of this are visible in Figure 7. The class may also include any wave gullies (Priestas and Fagherazzi, 2011) that are present. Ridge-runnels, if considered as analogous to spur and groove formations in coral reef systems, may be representative of a very sensitive region of the energy continuum and therefore be a rather plastic class in which small variations in energy are reflected in substantial morphological variability (Roberts et al., 1992). Exposed marshes account for only 14% of the margins within the ESN region and margin types are dominated by ramps(45%) and ridge-runnels (29%), with cliffs only comprising 26%. This may represent a tendency for marsh margins in high-energy environments to adopt a more dissipative form, particularly where wave action is of more significance than tidal flows. In sheltered environments (86%), however, cliffs are the most common landform, accounting for 52% of margins. Cliffs with complex planform morphology probably constitute an additional component that is subsumed within the ridge-runnel class, as discussed above. This contrasting landform prevalence between exposed and sheltered locations is likely to arise from the differences in geomorphic setting (wide, flat fronting mudflats in exposed settings compared to narrow, steep mudflats in more constrained channel systems) alongside differences in the balance between wave and tidal energy in terms of hydrodynamic exposure.

4.2 Relationship between margin type and morphodynamics

Overall, the our findings suggest a spatially-variable balance between the importance of external forcing and self-organised controls on landform evolution. Despite a dominance of external factors (exposure) there is clear evidence that margin configuration affects the interactions between landform and hydrodynamic conditions, modulating marsh system responses through time.

This study finds that the cliffed condition is a prevalent and probably relatively stable state in sheltered environments whereas its scarcity in exposed areas might suggest that it is a relatively transient landform state where incident energy conditions are higher. The lateral dynamism of these landforms is much less than for other marginal configurations irrespective of exposure, although cliffs do exhibit a greater tendency to be erosional (Mariotti and Fagherazzi, 2010). This, alongside the skewness statistics reported, supports the findings of Gunnell et al. (2013) and the assertion made by Fagherazzi (2013) that marsh advance tends to be

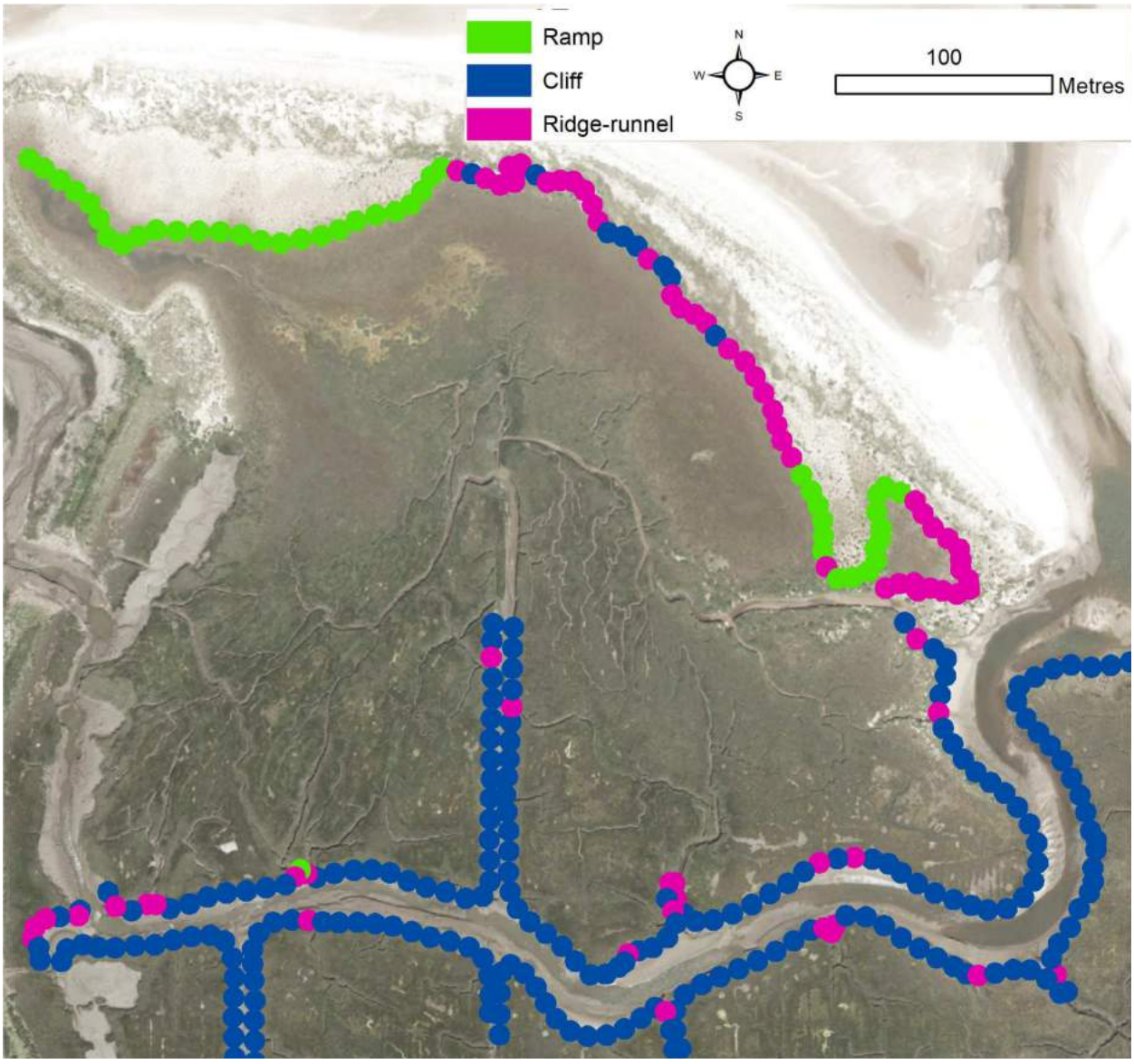

Figure 7: Detail showing aerial photography of a marsh area that exhibits a range of marginal characteristics and their associated classification. Titchwell, North Norfolk. Note the association of ridge-runnel classification with creek junctions and areas of added topographic complexity

more rapid than retreat and lends credence to Fagherazzi's assessment of century to millennium timescales for landscape cyclicity. The ensuing conclusion that, over management timescales of decades, changes are likely to be unidirectional is therefore tacitly supported also. The observations of advance associated with some cliffed margins, however, suggests re-establishment of vegetation in front of the scarp, constituting an observation of cyclicity similar to that made by van der Wal et al. (2008) that may also be related to persistence and recolonisation of slump blocks.

The finding that advance tends to be faster than retreat contrasts with the behaviour posited by van De Koppel et al. (2005) and Singh Chauhan (2009), in whose models retreat is rapid following criticality in a landform that has prograded gradually. It is possible that these models are appropriate for sandier systems such as Morecambe Bay, but not for the more cohesive East coast systems investigated here (Pringle, 1995). The apparent stability of marsh cliffs is, in part, a consequence of the geomorphic contexts in which they tend to occur. Cliffs dominate the banks of estuaries and channels where tidal flows may be stronger and prevent the accumulation of sediment channelward of the vegetated margin (limiting progradation), while slump blocks may protect the cliffs from erosion (Gabet, 1998; Allen, 2000). In more exposed areas, where mean wave energy is typically greater, landforms (i.e. ridge-runnels) exhibiting greater long-shore variability develop to dissipate the more laterally-variable cross-shore bi-directional currents. Perhaps not surprisingly, these landforms then also exhibit greater variability in morphological change over time.

4.3 Implications of findings

A central question in the development of the marginal classification methodology is that of scale. The relationship between the dimensions of the landscape features that are being measured, the resolution of the data from which measurements are taken and the size of the area over which they are sampled determines the nature and performance of any metrics derived. The empirical observation that a 10m sampling diameter (for a 25cm raster) is most informative of marsh marginal characteristics suggests that 10m is an appropriate scale at which to measure saltmarsh landscape attributes which is commensurate with the dimensions of the features themselves and the scale of their spatial variability. This has implications for future work in terms of desirable grid resolutions for numerical landscape models and also remotely-sensed products. Given the

increasing availability of very high resolution topography (e.g. from drones with pixel sizes of less than 1cm) the wider investigation of the influence of data resolution on morphometric indices would be valuable.

The findings presented here (particularly the paucity of cliffs in exposed environments) highlight the need for more research to address morphodynamics of other margin types. This is necessary to improve our understanding of their behaviours and hence the future of our marsh systems. We have also demonstrated that geomorphic setting has a significant impact on the nature of observed dynamics for all types of margin. Both empirical studies and numerical models therefore need to represent these contextual considerations much more explicitly than has hitherto been achieved, in order to avoid conflating dissimilar phenomena. Finally, the data presented above show that marginal changes can be very different depending on whether volumetric or lateral metrics are being considered. It is important to understand both types, but inferences made based on lateral dynamics may not necessarily be applicable to volumetric changes and *vice versa*.

5 Conclusions

This study has demonstrated that salt marsh margin landform types are statistically separable using a small set of indices derived from remotely sensed data. It therefore provides the first quantitative typology for marsh margins of which the authors are aware. Furthermore, the typology is based upon functional differences between landforms that are associated with different morphodynamic and ecosystem service attributes. This is demonstrated by the contrasting morphodynamic behaviours found to be associated with each margin type. We have demonstrated the value of applying quantitative approaches towards the classification of intertidal wetland margins as a means of improving our understanding of their self-organised dynamism, which may form a basis for inferences regarding future morphological change. This study has provided a large sample population across a diverse regional extent, from which it is possible to infer general behavioural tendencies of marsh margins from context and their 3-dimensional functional form. The results presented here therefore provide a robust quantitative basis for a rapid evaluation of likely system dynamism that may be useful to conservation practitioners or site managers.

6 Acknowledgements

We would like to acknowledge the contributions and support of the FAST consortium partners and are grateful for funding to support this work from the European Commission Seventh Framework Programme and the Isaac Newton Trust.

References

Allen, J. (1989). Evolution of salt-marsh cliffs in muddy and sandy systems: a qualitative comparison of British west-coast estuaries. *Earth Surface Processes and Landforms*, 14:85–92.

Allen, J. (1993). Muddy alluvial coasts of Britain: field criteria for shoreline position and movement in the recent past. *Proceedings of the Geologists' Association*, 104(4):241–262.

Allen, J. (2000). Morphodynamics of Holocene salt marshes: a review sketch from the Atlantic and Southern North Sea coasts of Europe. *Quaternary Science Reviews*, 19(12):1155–1231.

Baily, B. and Pearson, A. (2007). Change Detection Mapping and Analysis of Salt Marsh Areas of Central Southern England from Hurst Castle Spit to Pagham Harbour. *Journal of Coastal Research*, 26(7):1549–1564.

Balke, T., Stock, M., Jensen, K., Bouma, T. J., and Kleyer, M. (2016). A global analysis of the seaward salt marsh extent: The importance of tidal range. *Water Resources Research*, 52(5):3775–3786.

Baltz, D. M., Rakocinski, C., and Fleeger, J. W. (1993). Microhabitat use by marsh-edge fishes in a Louisiana estuary. *Environmental Biology of Fishes*, 36(2):109–126.

Cahoon, D. R. (2006). A review of major storm impacts on coastal wetland elevations. *Estuaries and Coasts*, 29(6):889–898.

Defina, A., Carniello, L., Fagherazzi, S., and D'Alpaos, L. (2007). Self-organization of shallow basins in tidal flats and salt marshes. *Journal of Geophysical Research*, 112(F3):F03001.

Dyer, K., Christie, M., and Wright, E. (2000). The classification of intertidal mudflats. *Continental Shelf Research*, 20(10):1039–1060.

Dyer, K. R. (1998). The typology of intertidal mudflats. *Geological Society, London, Special Publications*, 139(1):11–24.

Fagherazzi, S. (2013). The ephemeral life of a salt marsh. *Geology*, 41(8):943–944.

Fagherazzi, S., Gabet, E. J., and Furbish, D. J. (2004). The effect of bidirectional flow on tidal channel planforms. *Earth Surface Processes and Landforms*, 29(3):295–309.

Gabet, E. J. (1998). Lateral Migration and Bank Erosion in a Saltmarsh Tidal Channel in San Francisco Bay, California. *Estuaries*, 21(4):745.

Glancy, T. P., Frazer, T. K., Cichra, C. E., and Lindberg, W. J. (2003). Comparative patterns of occupancy by decapod crustaceans in seagrass, oyster, and marsh-edge habitats in a Northeast Gulf of Mexico estuary. *Estuaries*, 26(5):1291–1301.

Gray, A., Clarke, R., Warman, B., and Johnson, P. (1989). Prediction of marginal vegetation in a post-barrage environment. Technical report, nstitute of Terrestrial Ecology.

Gunnell, J. R., Rodriguez, A. B., McKee, B. A., P.M.J., H., D.R., C., S., T., K., S., A., L., and M., B. (2013). How a marsh is built from the bottom up. *Geology*, 41(8):859–862.

Leonardi, N., Defne, Z., Ganju, N. K., and Fagherazzi, S. (2016). Salt marsh erosion rates and boundary features in a shallow Bay. *Journal of Geophysical Research: Earth Surface*, 121(10):1861–1875.

Leonardi, N. and Fagherazzi, S. (2014). How waves shape salt marshes. *Geology*, 42(10):887–890.

Marani, M., Da Lio, C., and D'Alpaos, A. (2013). Vegetation engineers marsh morphology through multiple competing stable states. *Proceedings of the National Academy of Sciences*, 110(9):3259–3263.

Marani, M., D'Alpaos, A., Lanzoni, S., and Santalucia, M. (2011). Understanding and predicting wave erosion of marsh edges. *Geophysical Research Letters*, 38(21):n/a–n/a.

Mariotti, G. and Fagherazzi, S. (2010). A numerical model for the coupled long-term evolution of salt marshes and tidal flats. *Journal of Geophysical Research*, 115(F1):F01004.

Mariotti, G. and Fagherazzi, S. (2013). Critical width of tidal flats triggers marsh collapse in the absence of sea-level rise. *Proceedings of the National Academy of Sciences of the United States of America*, 110(14):5353–6.

McLoughlin, S. M., Wiberg, P. L., Safak, I., and McGlathery, K. J. (2015). Rates and Forcing of Marsh Edge Erosion in a Shallow Coastal Bay. *Estuaries and Coasts*, 38(2):620–638.

Minello, T. J., Zimmerman, R. J., and Medina, R. (1994). The importance of edge for natant macrofauna in a created salt marsh. *Wetlands*, 14(3):184–198.

Möller, I. and Spencer, T. (2002). Wave dissipation over macro-tidal saltmarshes : Effects of marsh edge typology and vegetation change. *Journal of Coastal Conservation*, 521(36):506–521.

Morris, J., Sundareshwar, P., Nietch, C., Kjerfve, B., and Cahoon, D. (2002). Responses of coastal wetlands to rising sea level . *Ecology*, 83(10):2869–2877.

Phelan, N., Shaw, A., and Baylis, A. (2011). The extent of saltmarsh in England and Wales : 2006 2009.

Priestas, A. M. and Fagherazzi, S. (2011). Morphology and hydrodynamics of wave-cut gullies. *Geomorphology*, 131(1-2):1–13.

Pringle, A. (1995). Erosion of a cyclic marsh in Morecambe Bay, northwest England. *Earth Surface Processes and Landforms*, 20:387–405.

Roberts, H., Murray, S., and Suhayda, J. (1975). Physical processes in a fringing reef system. *Journal of Marine Research*, 33:233–260.

Roberts, H. H., Wilson, P. A., and Lugo-Fernández, A. (1992). Biologic and geologic responses to physical processes: examples from modern reef systems of the Caribbean-Atlantic region. *Continental Shelf Research*, 12(7):809–834.

Rogers, J. S. and Monismith, S. G. (2014). Hydrodynamics of spur and groove formations on a coral reef. *Journal of Geophysical Research*, 118(April):145–160.

Roner, M., Alpaos, A. D., Ghinassi, M., Marani, M., Silvestri, S., and Franceschinis, E. (2016). Spatial variation of salt-marsh organic and inorganic deposition and organic carbon accumulation : Inferences from the Venice lagoon , Italy. *Advances in Water Resources*, 93:276–287.

Singh Chauhan, P. P. (2009). Autocyclic erosion in tidal marshes. *Geomorphology*, 110(3-4):45–57.

526 Suchrow, S. and Jensen, K. (2010). Plant species responses to an elevational gradient in German North Sea
527 salt marshes. *Wetlands*, 30(4):735–746.

528 Temmerman, S., Bouma, T., Van de Koppel, J., Van der Wal, D., De Vries, M., and Herman, P. (2007).
529 Vegetation causes channel erosion in a tidal landscape. *Geology*, 35(7):631.

530 Theiler, E., Himmelstoss, E., Zichichi, J., and Ergul, A. (2008). Digital Shoreline Analysis System (DSAS)
531 version 4.0An ArcGIS extension for calculating shoreline change: U.S. Geological Survey Open-File Report
532 2008-1278. Technical report, USGS.

533 Tonelli, M., Fagherazzi, S., and Petti, M. (2010). Modeling wave impact on salt marsh boundaries. *Journal*
534 *of Geophysical Research*, 115(C9):C09028.

535 Townend, I. H. (2008). Hypsometry of estuaries, creeks and breached sea wall sites. *Proceedings of the ICE*
536 *- Maritime Engineering*, 161(1):23–32.

537 Trevisani, S. and Rocca, M. (2015). MAD: robust image texture analysis for applications in high resolution
538 geomorphometry. *Computers & Geosciences*, 81:78–92.

539 van de Koppel, J., Bouma, T. J., and Herman, P. M. J. (2012). The influence of local- and landscape-scale
540 processes on spatial self-organization in estuarine ecosystems. *The Journal of experimental biology*, 215(Pt
541 6):962–7.

542 van De Koppel, J., van der Wal, D., Bakker, J. P., and Herman, P. M. J. (2005). Self-Organization and
543 Vegetation Collapse in Salt Marsh Ecosystems. *The American Naturalist*, 165(1):E1–E12.

544 van der Wal, D., Wielemaker-Van den Dool, A., and Herman, P. M. (2008). Spatial patterns, rates and
545 mechanisms of saltmarsh cycles (Westerschelde, The Netherlands). *Estuarine, Coastal and Shelf Science*,
546 76(2):357–368.

547 Whaley, S. D. and Minello, T. J. (2002). The distribution of benthic infauna of a Texas salt marsh in relation
548 to the marsh edge. *Wetlands*, 22(4):753–766.

Margin type	mean RMSE (m)	range (m)	CoV
Ridge-runnel	4.03	1.45	0.10
Cliff	0.54	0.09	0.06
Ramp	1.18	0.21	0.06

Table 1: Errors associated with identification and manual tracing of marsh margin locations based on panchromatic imagery

Type	Min	Max	Median	Mean	St. Dev	Skew	Kurt	n
HT								
All	-10.95	75.78	0.00	2.42	6.85	3.74	22.78	33287
ESN								
All	-6.10	9.30	-0.05	-0.10	0.88	0.77	16.49	15774
Ramp	-5.71	7.05	-0.08	-0.23	1.25	0.37	7.00	3166
Cliff	-5.40	8.05	-0.04	-0.04	0.55	1.10	40.15	7705
Ridge	-6.10	9.30	-0.07	-0.09	0.99	1.27	15.40	
ESN Exposed								
All	-5.41	9.30	-0.70	-0.82	1.36	0.96	8.30	2162
Ramp	-5.41	7.05	-1.01	-0.91	1.51	1.24	7.46	972
Cliff	-5.40	4.82	-0.35	-0.59	0.95	-1.11	7.51	571
Ridge	-5.11	9.30	-0.82	-0.89	1.41	1.21	9.21	619
ESN sheltered								
All	-6.10	9.07	-0.04	0.01	0.71	2.06	25.98	13612
Ramp	-5.71	5.57	-0.04	0.07	0.99	0.47	9.64	2194
Cliff	-4.99	8.05	-0.04	-0.01	0.47	3.49	59.43	7134
Ridge	-6.10	9.07	-0.05	0.02	0.85	2.29	21.31	4284

Table 2: Descriptive statistics for EPR (m y^{-1}) calculated across entire HT region, for ESN locations where paired margin classifications and change estimates are available, and sub-divided into exposed and sheltered ESN locations. St. Dev = Standard deviation, Skew = skewness, Kurt = Kurtosis, 'Ridge' denotes ridge-runnel

Class (i)	Class (ii)	95% CI LB	Diff (means)	95% CI UB	p-Value
		All ESN			
EPR					
ramp	cliff	-0.223	-0.178	-0.133	<0.001
ramp	ridge	-0.186	-0.137	-0.088	<0.001
cliff	ridge	0.002	0.041	0.081	0.034
Absolute EPR					
ramp	cliff	0.531	0.569	0.606	<0.001
ramp	ridge	0.246	0.287	0.328	<0.001
cliff	ridge	-0.315	-0.282	-0.249	<0.001
VCR					
ramp	cliff	-0.144	-0.104	-0.063	<0.001
ramp	ridge	-0.144	-0.101	-0.057	<0.001
cliff	ridge	-0.032	0.003	0.038	0.977
Absolute VCR					
ramp	cliff	0.070	0.105	0.140	<0.001
ramp	ridge	0.022	0.060	0.098	<0.001
cliff	ridge	-0.075	-0.045	-0.014	0.002
		ESN Exposed			
EPR					
ramp	cliff	-0.486	-0.311	-0.136	<0.001
ramp	ridge	-0.184	-0.014	0.157	0.981
cliff	ridge	0.105	0.297	0.489	<0.001
Absolute EPR					
ramp	cliff	0.536	0.668	0.799	<0.001
ramp	ridge	-0.012	0.116	0.244	0.086
cliff	ridge	-0.696	-0.552	-0.407	<0.001
VCR					
ramp	cliff	0.055	0.206	0.355	0.004
ramp	ridge	-0.030	0.117	0.263	0.149
cliff	ridge	-0.253	-0.088	0.077	0.423
Absolute VCR					
ramp	cliff	-0.328	-0.198	-0.068	<0.001
ramp	ridge	-0.321	-0.194	-0.068	<0.001
cliff	ridge	-0.139	0.004	0.147	0.998
		ESN Sheltered			
EPR					
ramp	cliff	0.035	0.077	0.119	<0.001
ramp	ridge	0.001	0.047	0.092	0.043
cliff	ridge	-0.64	-0.030	0.003	0.086
Absolute EPR					
ramp	cliff	0.313	0.350	0.387	<0.001
ramp	ridge	0.098	0.138	0.178	<0.001
cliff	ridge	-0.241	-0.212	-0.183	<0.001
VCR					
ramp	cliff	-0.004	0.035	0.073	0.087
ramp	ridge	-0.039	0.002	0.043	0.992
cliff	ridge	-0.063	-0.033	-0.002	0.032
Absolute VCR					
ramp	cliff	-0.044	-0.010	0.024	0.763
ramp	ridge	-0.054	-0.018	0.019	0.493
cliff	ridge	-0.034	-0.007	0.019	0.790

Table 3: Results of multiple comparison analysis for difference in means of EPR, absolute EPR, VCR and absolute VCR between margin classes with lower (LB) and upper (UB) bounds of the 95% confidence interval and associated p-values for pairwise tests. 'ridge' denotes ridge-runnel. Rows with significant differences at the 5% level are highlighted yellow